*Fire Safety Journal* **16** (1990) 213–227

# The Unloading of Building Materials Submitted to Fire

J. M. Franssen

Institut du Genie Civil, Université de Liège, Quai Banning 6, B-4000 Liège, Belgium

(Received 19 October 1989; revised version received 8 February 1990; accepted 28 February 1990)

*ABSTRACT*

*The unloading of building materials is considered in uniaxially oriented structures.*

*It is shown how the uncertainty encountered in numerical simulations between loading or unloading can be resolved when using the principle of Duhamel and assuming that the plastic strain is not affected by a temperature variation. A solution is also proposed to consider the inelastic behaviour of a material with a non-linear stress–strain relationship like the linear-elliptic one that is often used for steel.*

*The analysis of three composite steel–concrete elements tends to prove that the consideration of inelastic behaviour is not critical in simply supported beams. It seems to be of more importance in an hyperstatic beam and even more in a centrically loaded composite column.*

## NOTATION

| | |
|---|---|
| $t$ | Time |
| $T$ | Temperature |
| $u$ | Displacement |
| $\beta_p$ | Limit of proportionality |
| $\Delta$ | Difference |
| $\varepsilon_{cr}$ | Creep strain |
| $\varepsilon_o$ | Initial strain |
| $\varepsilon_{pl}$ | Plastic strain |
| $\varepsilon_r$ | Residual strain |

$\varepsilon_{th}$ Thermal strain
$\varepsilon_{tr}$ Transient strain
$\varepsilon_T$ Total strain
$\varepsilon_\sigma$ Stress-related strain
$\sigma$ Stress
$\sigma_y$ Yield strength

## 1 INTRODUCTION

Many materials show inelastic behaviour when tested beyond a certain stress (or strain) limit. If the applied strain exceeds this limit and then decreases, the relations between stresses and strains are not the same during the unloading as they were in the loading phase. This is the case for the usual building materials such as steel and concrete.

This paper is dedicated to linearly oriented structures (trusses, beams, columns, frames, etc.) where uniaxial situations prevail. Figure 1 illustrates the situation in a one-dimensional stress–strain diagram. It is usually observed that the unloading forms a straight line parallel to the loading curve at its origin.

The first point investigated here concerns the uncertainty between loading and unloading. Even at ambient temperature, when the material at a certain location in the structure has come to an equilibrium state represented by point A on Fig. 1, and the step-by step analysis of the structure is carried on, it is not at all certain that an increase of the applied load will result in an increase of the stress. Unloading could appear due to second order effects linked to large displacements, for example. Though continuous loading is generally the rule at ambient temperature, unloading is much more common in structures submitted to a fire, partly due to the more likely occurrence of large displacements but also to the thermal effects and their transient character, particularly in reinforced concrete and in composite steel–

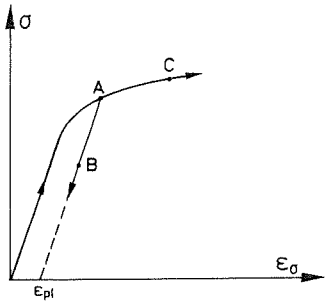


**Fig. 1.** Loading or unloading.

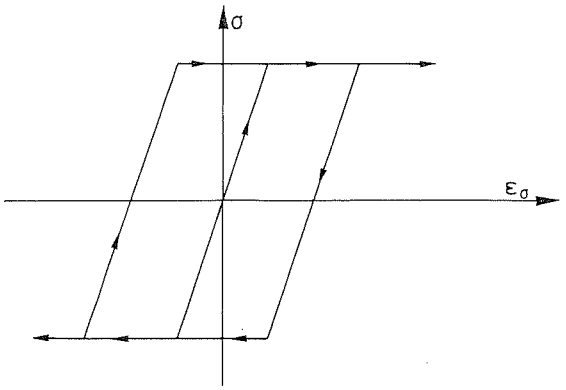


**Fig. 2.** Elastic perfectly plastic diagram.

concrete structures. Yet, a choice has to be made and it is of considerable importance in the formation of the stiffness matrix of the structure. The tangent modulus can be significantly lower if loading is assumed than if unloading is supposed. The wrong choice could lead to great out-of-balance forces and to a large number of iterations to restore the equilibrium. It could also lead the program into serious trouble and even to death, or at least its numerical equivalent, i.e. lack of convergence and premature end of the calculation. Not only is this problem more frequent in the case of a fire, but it is also more difficult to solve because of the variation of the stress–strain diagram due to the variation in temperature.

The second point to be focused upon is the way the unloading can be considered in the case of a stress–strain curve that is non-linear. If the stress–strain diagram is idealized as elastic perfectly plastic (Fig. 2), there is no question about the yield strength. It remains unchanged whatever the way of loading, provided that the temperature is constant. If a bilinear diagram with strain-hardening is considered (Fig. 3), and the positive yield strength has been increased by the loading, it is usually admitted that the negative yield strength is reduced accordingly and the elastic zone keeps the same magnitude though it has been shifted. This is the kinematic strain-hardening accounting for the Bausschinger effect. Let us now consider a diagram with an ellipsoidal part such as the one proposed by Rubert and Schaumann for steel.[1] Such an idealization seems to be favoured by most scholars for the appendices to the Eurocodes. A kinematic strain-hardening leads to the situation illustrated in Fig. 4, which is not very satisfactory if only because of the corner encountered at point D and being the source of additional numerical problems. An isotropic strain-hardening, on the contrary,

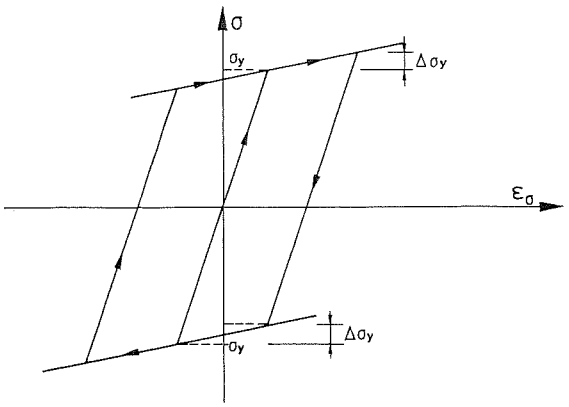


**Fig. 3.** Bilinear diagram.

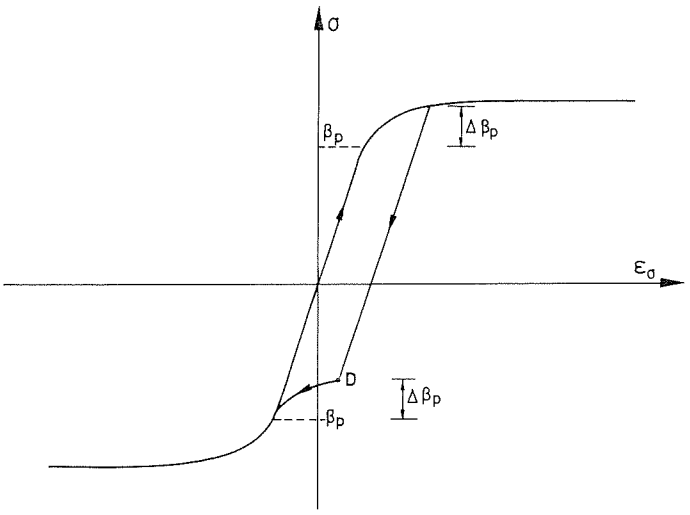


**Fig. 4.** Kinematic strain-hardening.

leads to the situation illustrated on Fig. 5, which does not seem much more satisfactory.

## 2 RESOLVING THE UNCERTAINTY

As far as uniaxial problems are concerned, the constitutive law of a heat submitted material can stand as follows:

$$\varepsilon_T = \varepsilon_\sigma + \varepsilon_o \tag{1}$$

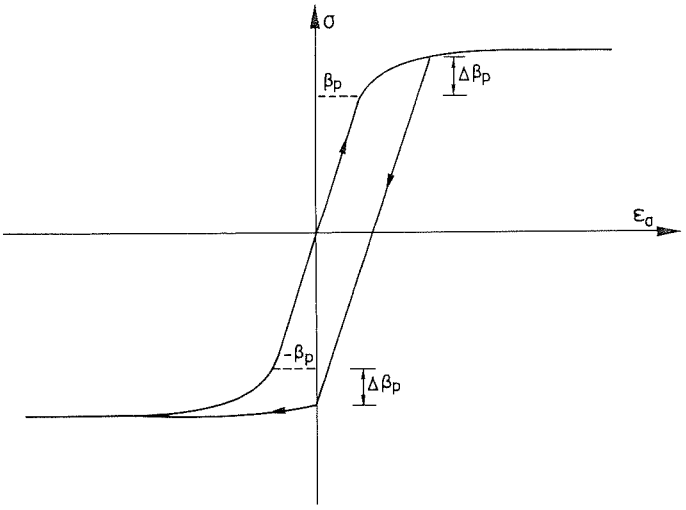


**Fig. 5.** Isotropic strain-hardening.

where

$\varepsilon_T$ = total strain, the one that is related to the displacement, and also the one that can be observed;
$\varepsilon_\sigma$ = the part of the total strain which induces stresses (usually called the stress-related strain);
$\varepsilon_o$ = initial strain.

The initial strain itself is made of different parts, depending on the proposed model. Among them.

$\varepsilon_{th}$ = thermal strain;
$\varepsilon_r$ = residual strain, due to the hot rolling of the profile, or to its welding;
$\varepsilon_{cr}$ = creep strain;
$\varepsilon_{tr}$ = transient strain.

The uncertainty between loading or unloading can be resolved by the use of two hypotheses.

## 2.1 Applicability of the principle of Duhamel[2]

The principle of Duhamel is usually applied for a material with a linear stress–strain relationship and without creep strain, transient strain or residual strain. Only the effect of thermal strain is considered. The idea, first established in Ref. 3, is to also apply this principle for the building materials submitted to fire.

Indeed, the relations governing the equilibrium, i.e. linking the external loads to the displacements by means of the stiffness matrix, are linearized in order to solve the problem by a step-by-step procedure. Incremental loads and displacements are linearly related through the tangent stiffness matrix.

In order to describe the way this principle can be applied, the following convention is used: a variable $A$ noted as $A^{m,n}$ means that it is considered at time increment $m$, at iteration $n$. $A^m$ is the variable at time increment $m$ after convergence has been obtained.

So, when a time increment $\Delta t = t^{m+1} - t^m$ is applied, corresponding to a temperature variation $\Delta T = T^{m+1} - T^m$ applying the principle of Duhamel is equivalent to set

$$\Delta u^{m+1,1} = 0 \tag{2}$$

where $u$ = displacement.

Equation (2) leads to

$$\Delta \varepsilon_T^{m+1,1} = 0 \tag{3}$$

and, through eqn (1), to

$$\Delta \varepsilon_\sigma^{m+1,1} = -\Delta \varepsilon_o^{m+1,1} \tag{4}$$

The value of $\Delta \varepsilon_o^{m+1,1}$ must be calculated explicitly, i.e. depending on $\sigma^m$. There is no difficulty for the thermal and residual strain. Explicit models also exist for the creep and transient strain (see Ref. 4, based on $\sigma^m$ and $\bar{T}^{m+1} = (T^{m+1} + T^m)/2$).

The value $\varepsilon_\sigma^{m+1,1}$ is then calculated according to

$$\varepsilon_\sigma^{m+1,1} = \varepsilon_\sigma^m + \Delta \varepsilon_\sigma^{m+1,1} \tag{5}$$

## 2.2 The plastic strain is not affected by a temperature variation

The plastic strain is the strain that would remain if the stress were decreased down to zero (Fig. 1).

This second hypothesis was already present in Ref. 5, though Forsen did not use it to resolve the uncertainty. Figure 6 shows what the stress–strain diagram at $T^{m+1}$ would be if $\varepsilon_{pl}^{m+1,1} = \varepsilon_{pl}^m$. The value $\varepsilon_\sigma^{m+1,1}$ being calculated by eqn (5), $\sigma^{m+1,1}$ and its associated tangent modulus are immediately found on this diagram.

In the particular case of Fig. 6, $\sigma^{m+1,1}$ is on the loading part of the diagram. The integration of the stresses provides the out-of-balance forces of iteration 1, whereas the integration of the tangent moduli provides the tangent stiffness matrix. Those quantities are now used to derive the incremental displacement $\Delta u^{m+1,2}$ and the incremental strain

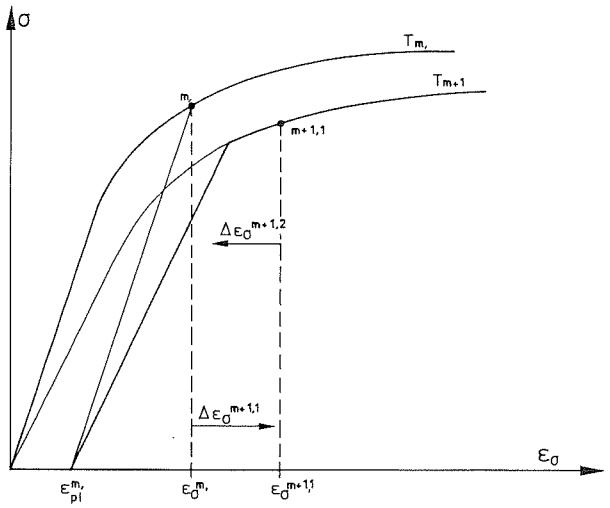


**Fig. 6.** Resolving the uncertainty.

$\Delta\varepsilon_\sigma^{m+1,2}$. The iterative process can go on, considering that $\Delta\varepsilon_\sigma^{m+1,i} = 0$ for $i > 1$. Of course, $\varepsilon_{pl}^{m+1}$ is recalculated only after the equilibrium $m+1$ has been reached, in order to avoid the so-called 'false unloadings' (i.e. unloadings that would occur during the iteration process but would not correspond to the situation that is found when convergence is obtained).

## 3 NON-LINEAR STRAIN-HARDENING IN STEEL

The developments of Section 2 still stand, whether the stress–strain diagram is bilinear or non-linear. What now if an elliptic diagram is used and the material first begins to yield in one direction (say, in compression) then undergoes an unloading important enough to make it yield in the opposite direction (in tension)?

The discussion is first based on a diagram at constant temperature. Some explanations will be given later on how to handle the problem in the case of varying temperature. In the following discussion, the hypothesis, the main results and the limitations will be pointed out, but not all of the developments will be detailed.

The main hypothesis is that the stress–strain behaviour of steel can be represented by the generalized Saint-Venant's model, i.e. the association (in parallel) of several elementary elastic–plastic models. Just as a multi-linear stress–strain diagram can result from such a generalized Saint-Venant's model with a finite number of elementary

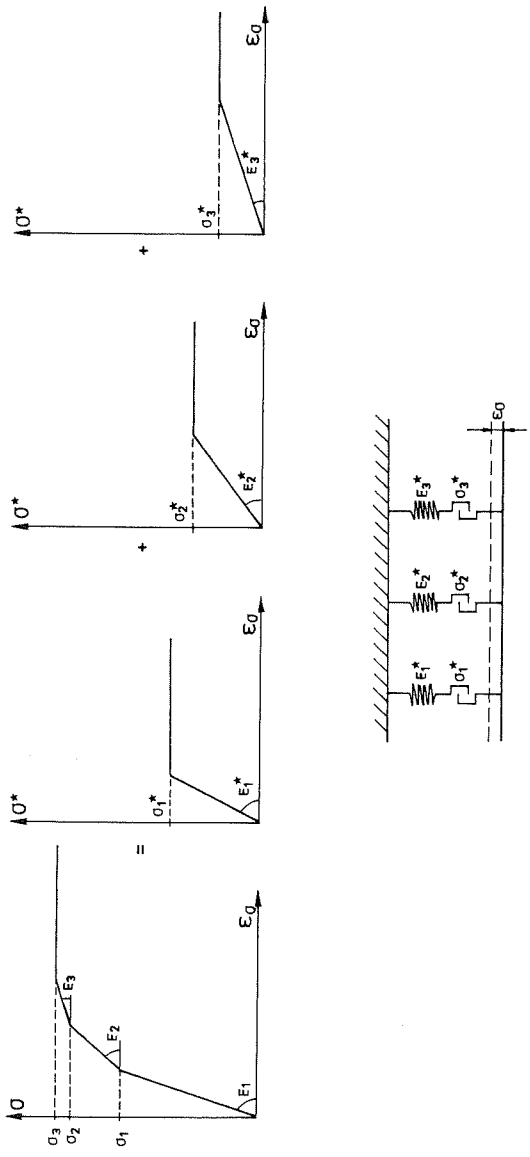


**Fig. 7.** Generalized Saint-Venant's model.

models (Fig. 7), a continuous non-linear stress–strain diagram can result from a generalized Saint-Venant's model with an infinite number of elementary models. For the multi-linear law, the characteristics $E_i^*$ and $\sigma_i^*$ of the elementary models are directly related to, and can be calculated from the characteristics $E_i$ and $\sigma_i$ of the total model. For a continuous law, it is also possible to derive from the loading curve of the total model, the characteristics of the elementary models representing it.

It can be shown that such a model follows the rule of Masing, i.e. the unloading curve results from a polar scaling of the loading curve. On Fig. 8, a loading up to $P$ is followed by an unloading. It occurs linearly up to $M$, with a linear stress range of $2\beta_p$. From that point, the unloading curve results from a polar scaling of the loading curve, $P'$ (the symmetric of $P$) being the pole. The ratio of the polar scaling is 2. The unloading curve reaches the loading curve tangentially at point $P'$. If the unloading goes further, the unloading and the loading curves are the same.

All that is required in addition to the loading curve to draw the complete stress–strain history, is the position of point $P$, the maximum level reached during the loading phase. This is true provided that, either only one unloading phase follows the loading phase (Fig. 9(a)), or cyclic loading occurs with always increasing stress levels (Fig. 9(b)). This, however, would not be true and more variables would be needed

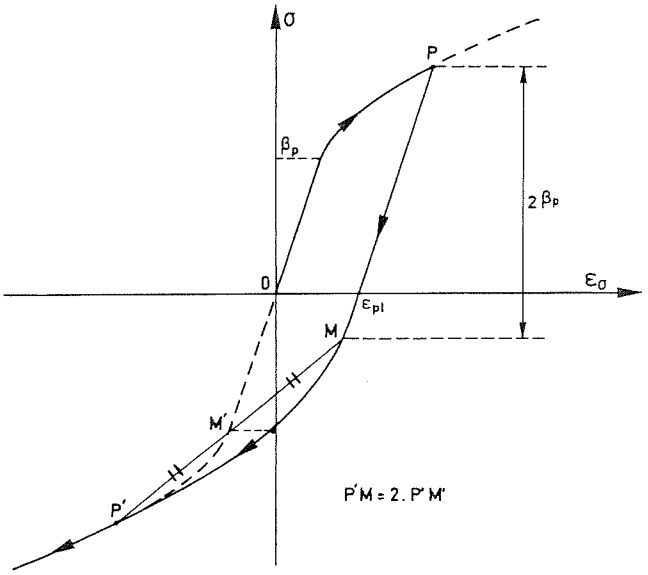


**Fig. 8.** Masing's rule.

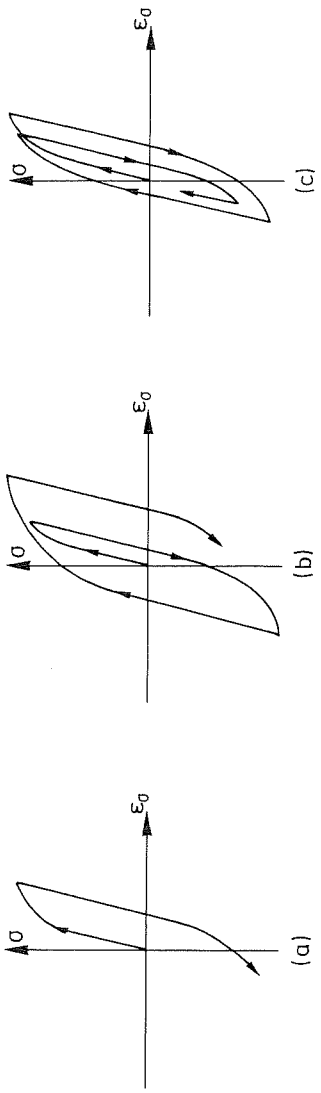


**Fig. 9.** Different possibilities.

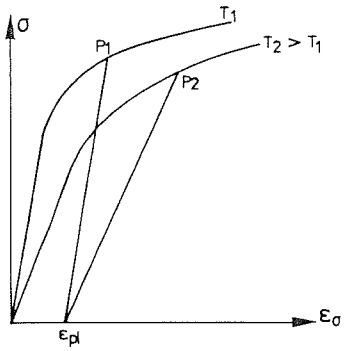


**Fig. 10.** Varying temperature.

in case of cyclic loading with decreasing stress levels (Fig. 9(c)). Yet, this is not a limitation in the case of a usual building structure submitted to a fire, where the situation in Fig. 9(a) will never be exceeded (i.e. cyclic loading will not be encountered).

In the case of varying temperature, the second hypothesis (Section 2.2) will be applied, i.e. the plastic strain is not affected by a temperature distribution. This means that, in fact, the plastic strain instead of the maximum stress level is the variable describing the complete stress–strain history in the case of varying temperature. The point $P$ is recalculated after each temperature increase, depending on $\varepsilon_{pl}$ (Fig. 10).

## 4 INFLUENCE OF THE UNLOADING EFFECT

Is it of any importance to consider the inelastic behaviour of building materials? Could not an elastic approximation be sufficient? It must be quoted that various authors such as Lie and Lin[6] for reinforced concrete columns, Quast, Hass and Rudolph[7] for composite elements and Wittbecker[8] for composite frames, do not consider the inelastic behaviour. On the other hand, FIRES-RC, one of the first computer programs for the behaviour of reinforced concrete elements, first established with an elastic model by Bizri, has quickly been transformed to accept an inelastic model.[9]

The hypotheses described in Sections 2 and 3 have been used in the program CEFICOSS. This program has been developed at the University of Liège[10] in close collaboration with ARBED[11] to simulate the fire behaviour of composite plane frames. The initial strain (see eqn (1)) is made of the thermal and residual strains, which means that creep is considered implicitly in the stress-related strain.

The first example to be calculated is a simply supported composite beam (HE 300 AA profile with concrete and 4 $\phi$ 25 re-bars between the flanges, a collaborating slab with a thickness of 14 cm). It has been calculated first with purely elastic materials and then taking the unloading into account as mentioned previously. No difference in the results is observed during the first phase of the calculation. As the calculation continues, the case with the elastic materials has a slightly greater deflection (6% greater when L/30 is obtained). No difference is observed concerning the failure time.

The second example is similar to the first one except that the rotation at one end of the beam is fixed. In this case, it is known that the negative bending moment at the support first increases because of the thermal stresses and then slowly decreases as the thermal gradients become less and less severe.

When the unloading effects are considered, the simulation runs quite well with an average of four iterations at every time step (usually 2 min) and the failure being obtained after 178 min 30 s. At that moment, the deflection is 39 cm (L/15) and the minimum eigenvalue of the stiffness matrix is 0·003, which indicates that the ultimate bearing capacity of the beam is really obtained.

When elastic materials are considered, the deflections are somewhat greater (5%), though not dramatically. More significant is the fact that it is impossible for the program to reach an equilibrium state after 123 min 30 s, even with a time step as short as 7·5 s. The deflection being only 14 cm (L/43) and the minimum eigenvalue of 0·023, indicates that this is not the real failure time of the beam, but a numerical failure due to the high yielding of materials at the support. At the support, materials are on the flat top of the stress–strain diagrams and convergence cannot be obtained.

The last example is a centrically loaded composite column (HE 300 A profile with concrete and 4 $\phi$ 25 between the flanges). The load is 350 kN and the buckling length 8 m (buckling around the weak axis). Due to the severity of the thermal stresses, important parts of the flanges yield. Yet, after 50 min, unloading takes place in the flanges and though temperatures are high, the elastic modulus in those zones is significant enough, if considered, to influence the stiffness of the column. It can be noticed in Fig. 11 that the lateral displacement is very dependent on the unloading effect and this, combined with the second order effects, has an influence on the failure time. The shape of both curves of Fig. 11 as well as the minimum eigenvalue of the stiffness matrix ($\approx$0·001) clearly indicates that 87 min 30 s and 101 min 30 s really correspond to the failure times. In this particular case, not taking the unloading effects amounts to neglecting 14% of the fire resistance of the column.

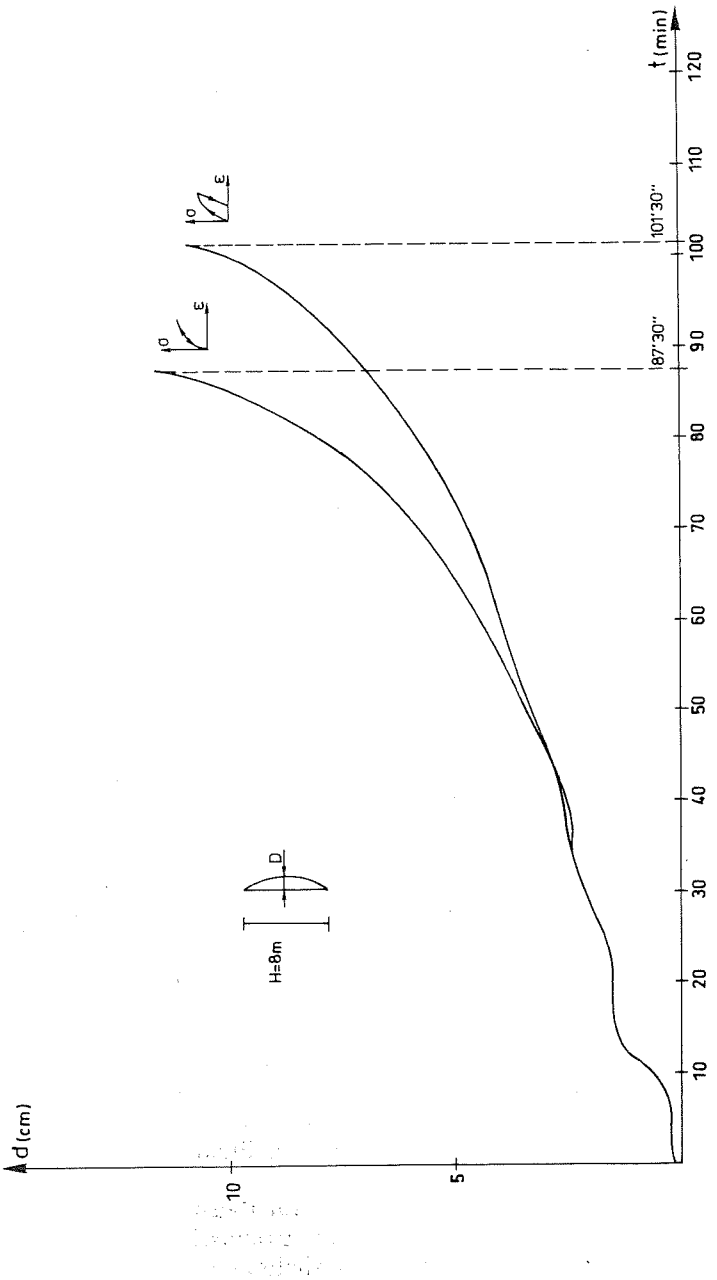


**Fig. 11.** Buckling of a composite column.

## 5 CONCLUSIONS

The normal conclusion of this paper should be to prove, by one or two well-chosen examples of real fire tests, that reality can only be simulated when the solutions proposed by the author are used, and that any attempt to calculate with other solutions would be futile. Indeed, the simulation of the two beams of Section 4 is closer to reality when the unloading is considered (the column has no real counterpart).

The author nevertheless decided not to do that, knowing too well that two other well-chosen examples could prove exactly the contrary.

The aim of this paper was to show that

(1) reasonable solutions can be found to simulate the unloading effects even for non-linear stress–strain relationships;
(2) those solutions are based on physically meaningful (though debatable) hypotheses rather than guesses;
(3) the consideration of the unloading effects can be of a significant influence. It can reasonably be foreseen that this influence will be even more significant when fire in complete structures as well as natural fires with cooling phases will be more and more commonly analysed in the fire engineering of a structure.

## REFERENCES

1. Rubert, A. & Schaumann, P., Stahlbau—temperaturabhängige werkstoffeigenschaften von Baustahl bei Brandbeanspruchung, **54** (1985) H3, 81–6.
2. Duhamel, J., Mémoires par divers savants—Mémoire sur le calcul des actions moléculaires développées par les changements de températures dans les corps solides. **5** (1838) 440–98.
3. Dotreppe, J. C., Méthodes numériques pour la simulation du comportement au feu des structures en acier et en béton armé. Thèse d'agrégation de l'enseignement supérieur, Université de Liège, 1980.
4. Anderberg, Y. & Therlandersson, S., Stress and deformation characteristics of concrete at high temperatures. Lund Institute of Technology *Bulletin 54,* 1976.
5. Forsen, N. E., A theoretical study on the fire resistance of concrete structures. The Norwegian Institude of Technology, 1982.
6. Lie, T. T. & Lin, T. D., Fire Performance of Reinforced Concrete Columns. *Fire Safety: Science and Engineering,* Philadelphia, ASTM STP **882** (1985) 176–205.
7. Quast, U., Hass, R. & Rudolph, K., Institut für Baustoffe, Massivbau und Brandschutz der Technischen Universität Braunschweig—STABA—F: Berechnung des Tag—und Verformungsverhaltens von einachsig gespannten Bauteilen unter Feuerangriff. 1984.

8. Wittbecker F.-W., Bergische Universitat GH Wuppertal—Gesamttragverhalten thermisch instationär beanspruchter Stahlverbundkonstrucktionen. Helft 1, 1987.
9. Becker, J. & Bresler, B., FIRES-RC. A Computer Program for the *FI*re *RE*sponse of *S*tructures-*R*einforced *C*oncrete Frames. Fire Research Group, Dept. of Civil Engineering, University of California Report No. UCB FRG 74–3, 1974.
10. Franssen, J.-M., Etude du comportement au feu des structures mixtes acier-béton. Thèse de doctorat, Université de Liège, Collection des Publications de la F.S.A., no. 111, 1987.
11. Schleich, J. B., C. E. C., REFAO-CAFIR, Computer Assisted Analysis of the Fire Resistance of Steel and Composite Concrete—Steel Structures. Final Report EUR 10828 EN, 1987.